

Exciton-Plasmon States in Nanoscale Materials: Breakdown of the Tamm–Dancoff Approximation

Myrta Grüning,^{*,†,¶} Andrea Marini,[‡] and Xavier Gonze[†]

European Theoretical Spectroscopy Facility, Université Catholique de Louvain, Belgium,
and European Theoretical Spectroscopy Facility, Università di Roma “Tor Vergata”, Italy

Received December 9, 2008; Revised Manuscript Received July 14, 2009

ABSTRACT

Within the Tamm–Dancoff approximation, *ab initio* approaches describe excitons as packets of electron–hole pairs propagating only forward in time. However, we show that in nanoscale materials excitons and plasmons hybridize, creating exciton–plasmon states where the electron–hole pairs oscillate back and forth in time. Then, as exemplified by the *trans*-azobenzene molecule and the carbon nanotubes, the Tamm–Dancoff approximation yields errors larger than the accuracy claimed in *ab initio* calculations. Instead, we propose a general and efficient approach that avoids the Tamm–Dancoff approximation, correctly describes excitons, plasmons, and exciton–plasmon states, and provides a good agreement with experimental results.

The *ab initio* Bethe–Salpeter (BS)¹ equation allows the accurate calculation of the polarization function of many physical systems without relying on external parameters. Within this framework neutral excitations are described as combination of electron–hole (e–h) pairs of a noninteracting system. However for nanoscale materials, the huge number of e–h pairs involved makes the solution of the BS equation extremely cumbersome. Consequently, the increasing interest in the excitation properties of such materials has justified the use of ad-hoc approximations. The most important and widely used is the Tamm–Dancoff approximation (TDA)² where only positive energy e–h pairs are considered. Within the TDA, the interaction between e–h pairs at positive and negative (antipairs) energies is neglected, and only one e–h pair is assumed to propagate in any time interval. The main advantage of the TDA is that the non-Hermitian BS problem reduces to a Hermitian problem that can be solved with efficient and stable iterative methods.³

In Solid State Physics, a major field of application of the BS equation, the success of the TDA is based on the sharp distinction between excitonic and plasmonic excitations. Excitons are localized packets of e–h pairs bound together by the Coulomb attraction and are observed in optical absorption experiments. Plasmons instead are delocalized collective oscillations of the electronic density that induce a

macroscopic polarization effect and are observed in electron energy loss (EEL) experiments. In contrast to the case of excitons, the TDA is known to misdescribe plasmons in solids⁴ as the density oscillations involve the excitation of e–h antipairs. Nevertheless, the success in describing optical absorption of solids and the remarkable numerical advantages have motivated the application of the TDA to very different systems. Nowadays the BS equation within the TDA is becoming a standard tool to study excitations in nanostructures^{5,6} and in molecular systems.⁷

In this work, we argue that for confined systems, such as nanotubes or π -conjugated molecules, the excitations appearing in the response function show a mixed excitonic–plasmonic behavior. As a consequence the e–h pair–antipair interaction becomes crucial and the TDA does not hold anymore. A paradigmatic example is the *trans*-azobenzene molecule, where the TDA overestimates the position of the main peak in the polarizability spectrum by ~ 0.2 eV. This error is larger than the claimed accuracy in *ab initio* calculations. Even more intriguing is the case of carbon nanotubes that, because of the quasi-one-dimensional (1D) structure, behave either as extended or isolated system depending on the polarization of the perturbing field. Thus, for transverse perturbations the excitons acquire a plasmonic nature and the TDA overestimates the position of the π plasmon peak appearing in both absorption and EEL spectra by almost 1 eV. The TDA also predicts the main photoabsorption peak to red shift as the angle ϕ between the light polarization and the tube axis goes from 0° (longitudinal polarization) to 90° (transverse polarization). This is in stark

* To whom correspondence should be addressed. E-mail: myrta@teor.fis.uc.pt.

[†] Université Catholique de Louvain.

[‡] Università di Roma.

[¶] Present address: Centre for Computational Physics and Physics Department, University of Coimbra, Rua Larga 3004-516 Coimbra, Portugal.

contrast with the experimental results where the main peak is observed to blue shift as ϕ increases.

By exploiting the symmetry properties of the BS kernel, we devise a robust and efficient iterative approach to calculate the frequency-dependent response, beyond the TDA. This approach benefits from the same numerical advantages of Hermitian techniques, correctly describes excitons, plasmons, and exciton-plasmon states, and provides a good agreement with the experimental results.

To introduce and understand the reasons beyond the breakdown of the TDA, we need to study in detail the structure of the BS equation. This is commonly rewritten as a Hamiltonian problem,⁸ by expanding the single particle states in the Kohn–Sham basis. Then, the BS Hamiltonian H is a matrix in the Fock space of the e–h pairs $|eh\rangle$ and antipairs $|\bar{h}\bar{e}\rangle$, and it has the block-form

$$H = \begin{pmatrix} R & C \\ -C^* & -R^* \end{pmatrix} \quad (1)$$

The resonant block R is Hermitian and the coupling block C is symmetric (see Appendix B of ref 8). The dielectric function $\varepsilon(\omega)$ is written in terms of the resolvent of H , $(\omega - H)^{-1}$, as $\varepsilon(\omega) = 1 - (8\pi/\Omega)\langle P | (\omega - H + i0^+)^{-1} | P \rangle$, where Ω is the simulation volume. In the limit of large Ω the polarizability is given by $\alpha(\omega) \propto \varepsilon(\omega)$. $|P\rangle$ is a ket whose components along the $|eh\rangle$ space are the optical oscillators $\langle P | eh \rangle \sim \langle e | \vec{d} \cdot \vec{\xi} | h \rangle$, with \vec{d} the electronic dipole, and $\vec{\xi}$ the light polarization factor.

The matrix elements of R and C in eq 1 are, respectively,

$$R_{hh'}^{ee} = E_{eh} \delta_{ee'} \delta_{hh'} + \langle eh | W - 2\bar{V} | e'h' \rangle$$

and

$$C_{hh'}^{ee} = \langle eh | W - 2\bar{V} | \bar{h}'\bar{e}' \rangle$$

E_{eh} is the energy of the independent e–h pair, W is the statically screened e–h attraction, and \bar{V} is the bare Coulomb interaction without the long-range tail.⁸ Note that Time-Dependent Density Functional Theory,⁹ another ab initio method for calculating the polarization function of physical systems, widespread within the computational physics and chemistry community, possesses a Hamiltonian formulation of the same form as eq 1. The only difference with respect to the BS equation is that W is replaced by $-2f_{xc}$, with f_{xc} the exchange-correlation kernel. As the approach proposed in this work does not depend on the specific expression for the R and C matrix elements, it is valid for both the BS and the time-dependent density functional theory equations.

The TDA assumes that the effect induced by the e–h antipairs is negligible. Consequently, the C block, that couples pairs and antipairs, is neglected, and the Hamiltonian H is approximated by R . The coupling described by C is dominated by the contribution arising from the bare Coulomb interaction \bar{V} . This term, called Hartree contribution, measures the degree of inhomogeneity of the electronic density.

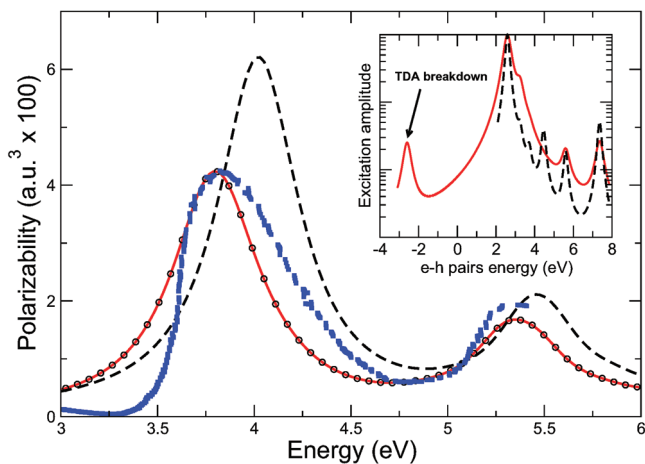


Figure 1. Dynamical polarizability of the *trans*-azobenzene molecule calculated within the BS equation either by using the full Hamiltonian (red solid line) or the TDA (dashed line) compared with the experimental data (blue squares).¹² To demonstrate the accuracy of the iterative approach, the spectrum obtained by diagonalization of the spectrum (circles) is also shown. The amplitude function (inset) of the most intense peak of the polarizability (see text) differs dramatically in the TDA and in the full Hamiltonian. The TDA misses of an important contribution from the spatially extended e–h antipairs with energy ~ -2.7 eV.

The larger this inhomogeneity, the stronger the corresponding polarization and the induced local fields that counteract the external perturbing field. Therefore, the inhomogeneity of the electronic density and the strength of local fields discriminate whether an excitation is well described by the TDA. Furthermore the TDA is known to fail for plasmonic excitations⁴ that, causing an oscillation of the density, involve the creation of e–h pairs and antipairs.

The electronic density of confined systems, like molecules and nanostructures, is typically strongly inhomogeneous. Moreover the excitons can be spread all over the molecule, involving the excitations of most of the electrons. Thus, in contrast to solids, it is not possible to distinguish between excitonic and plasmonic excitations, and the arguments commonly used to sustain the TDA fail.

Indeed, the striking failure of the TDA is clearly demonstrated by the dynamical polarizability $\mathcal{F}[\alpha(\omega)]$ of *trans*-azobenzene, calculated within the BS equation.^{10,11} In Figure 1, we compare the calculated $\mathcal{F}[\alpha(\omega)]$, either using the TDA or by solving the full BS H eigenproblem, with the experimental spectrum.¹² The spectrum obtained from the solution of the full Hamiltonian well reproduces the position of the experimental peaks and the relative intensity. Instead the TDA blue shifts by 0.2 eV the position and overestimates the intensity of the main peak.¹³ The reason for this failure can be understood by looking at the amplitude function $A^\lambda(\omega)$ corresponding to the eigenstate $|\lambda\rangle$ of H , defined as

$$A^\lambda(\omega) = \sum_{\eta=\{eh\},\{\bar{e}\bar{h}\}} |\langle \eta | \lambda \rangle|^2 \delta(\omega - E_\eta)$$

The $A^{\lambda_{\max}}$ function for the state λ_{\max} corresponding to the most intense peak of the α spectrum is shown in the inset of Figure

1. In the TDA, the λ_{\max} state is decomposed only in e–h pairs with $E_{\eta} > 0$. However, the solution the full Hamiltonian reveals an important contribution from the e–h antipair with energy ~ -2.7 eV. This term corresponding to a spatially extended $\pi^* \rightarrow \pi$ transition and neglected in the TDA, causes a dramatic overall redistribution of weights, and thus changes the character of the excitation.

The example of the *trans*-azobenzene makes clear that a proper description of the electron–electron correlation in confined systems requires the solution of the full BS Hamiltonian, beyond the TDA. However, for larger nanostructures with many degrees of freedom, the size of the H matrix can be as large as $10^6 \times 10^6$ and consequently the problem is impossible to treat if not using iterative methods. The TDA reduces H to a Hermitian Hamiltonian and makes possible to use the efficient and stable Hermitian iterative approaches.³ Therefore we need an iterative approach to calculate the resolvent of the full non-Hermitian Hamiltonian H as efficient and stable as for the Hermitian case.

In what follows, we show that it is indeed possible to design such an iterative approach by observing that H belongs to a class of non-Hermitian Hamiltonians with a real spectrum, that is, real eigenvalues. As established by Mostafazadeh,¹⁴ the reality of the spectrum is related to the existence of a positive-definite inner product with respect to which the Hamiltonian is Hermitian. We show that for the BS Hamiltonian, and in general for all the Hamiltonians of this form, this inner product does exist (thus the spectrum is real) and, more importantly, it is explicitly known. The knowledge of this product allows one to conveniently transform the iterative approach designed for the Hermitian TDA Hamiltonian to treat the full non-Hermitian Hamiltonian.

Following Zimmermann¹⁵ we can write H as the product of two noncommuting Hermitian matrices

$$H = F\bar{H} = \begin{pmatrix} 1 & 0 \\ 0 & -1 \end{pmatrix} \begin{pmatrix} R & C \\ C^* & R^* \end{pmatrix} \quad (2)$$

One can check that $\bar{H}H = H^*\bar{H}$. This key property of H is called \bar{H} -pseudo-Hermiticity.¹⁶ Through the \bar{H} operator, we can define a positive-definite \bar{H} -inner product¹⁷ $\langle \cdot | \cdot \rangle_{\bar{H}} := \langle \cdot | \bar{H} \cdot \rangle$, and a corresponding \bar{H} -expectation value $\langle \cdot | O | \cdot \rangle_{\bar{H}} := \langle \cdot | \bar{H} O | \cdot \rangle$. With respect to this \bar{H} -expectation value, H is Hermitian as can be verified by using the \bar{H} -pseudo-Hermiticity

$$\langle \nu | H | \nu' \rangle_{\bar{H}} = \langle \nu' | H^* \bar{H} | \nu \rangle^* = \langle \nu' | \bar{H} H | \nu \rangle^* =: \langle \nu' | H | \nu \rangle_{\bar{H}}^* \quad (3)$$

It follows that the \bar{H} -expectation value of the resolvent of H , $(\omega - H)^{-1}$, is Hermitian as well. Then, to evaluate $\langle P | (\omega - H)^{-1} | P \rangle$ and thus $\varepsilon(\omega)$, we rewrite it in terms of the Hermitian \bar{H} -expectation value by using the completeness relationship $I = \sum_k |q_k\rangle\langle q_k| \bar{H}$

$$\langle P | (\omega - H)^{-1} | P \rangle = \sum_k \langle P | q_k \rangle \langle q_k | (\omega - H)^{-1} | P \rangle_{\bar{H}} \quad (4)$$

where $\{|q_k\rangle\}$ is a complete basis, orthonormal with respect to the \bar{H} -inner product. The $\langle q_k | (\omega - H)^{-1} | P \rangle_{\bar{H}}$ are conveniently calculated within the standard Lanczos–Haydock (LH) iterative method,¹⁸ the same used in the TDA Hermitian case,¹⁹ provided that the \bar{H} -inner product replaces the standard one. The LH method recursively builds the $\{|q_k\rangle\}$ basis in which H is represented by a one-dimensional semi-infinite chain of sites with only nearest-neighbors interactions. For such a system the evaluation of the matrix elements of $(\omega - H)^{-1}$ reduces to the calculation of a continued fraction.¹⁸

This approach allows us to treat systems as large as commonly done within the TDA, but using the full Hamiltonian. Computationally, it requires a single matrix-vector multiplication at each iteration, as in the Hermitian case.²⁰ Since $\langle P | (\omega - H)^{-1} | P \rangle$ in eq 4 is converged after a number of iterations much smaller than the dimension of H , this method is far more efficient than performing the diagonalization of the Hamiltonian. Specifically, for the *trans*-azobenzene, the number of operations performed in the diagonalization is about 2 orders of magnitude larger than in our approach,²¹ while the results are indistinguishable (Figure 1).

As an application we consider the frequency-dependent response of carbon nanotubes (CNTs). The latter is characterized in the near-infrared and visible region by localized interband transitions specific of the particular CNT diameter and chirality,²² and by a broad intense peak in the ultraviolet (UV) region above 4 eV. Recently several experimental studies (see e.g., refs 23 and 24) have been focused on the UV region, trying to give simple (though sometimes contradictory) interpretations of the observed peak in terms of interband transitions, bulk, and surface plasmons. On the other hand, so far ab initio BS studies^{6,25} have been limited to the excitonic effects appearing below 4 eV and mostly for longitudinal polarized light. In fact, calculations of the optical response to perturbing fields above 4 eV are extremely challenging, as the collective character of the excitation requires the inclusion of a huge number of e–h pairs. Using the method proposed in this work we were able to include up to $\sim 1.4 \times 10^5$ e–h pairs in the solution of the BS equation without using the TDA in order to calculate the polarization dependence of response properties of CNTs for energies up to 8 eV.

Figure 2 shows the photoabsorption cross section, $\sigma \propto \omega \mathcal{I}[\varepsilon^{-1}(\omega)]$,⁸ obtained experimentally for aligned CNTs bundles²³ (top panel) or calculated within the BS equation (middle panel, full solution; bottom panel, TDA) for an isolated zigzag (8,0) CNT.^{10,26} Experimentally the prominent feature of the spectrum is the broad intense peak above 4 eV. This peak is blue shifted by about 0.7 eV when changing the light polarization from parallel ($\phi = 0^\circ$) to perpendicular to the tube axis ($\phi = 90^\circ$), with ϕ being the angle between the perturbing field and the tube axis. This polarization dependence has also been observed in momentum dependent EEL²⁴ on individualized CNTs, and it does not depend on the particular aggregation state of the CNTs, being related to their graphitic nature.

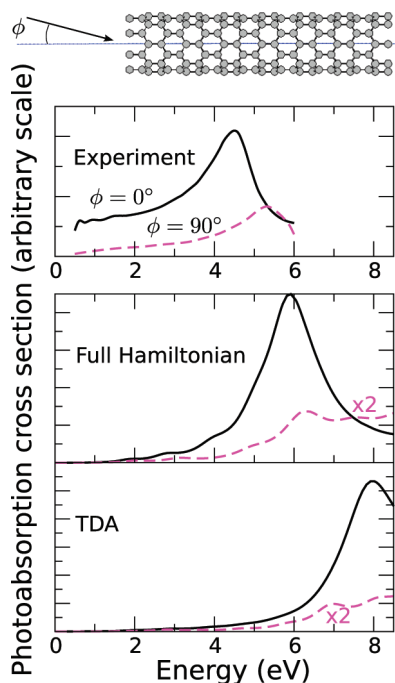


Figure 2. Photoabsorption cross section spectra of zigzag (8,0) CNT calculated within the BS equation either by using the full Hamiltonian (middle panel) or the TDA (bottom panel) for light polarized parallel (black continuous line) or perpendicular (magenta dashed line, intensity scaled by a factor 2) to the tube axis. The top panel shows experimental results from ref 23 obtained for a film of aligned CNTs. Going from longitudinal to transverse polarization a blue shift of ~ 0.7 eV of the main peak position is observed. Consistently,²⁷ the full Hamiltonian calculations predict a blue shift of about 0.5 eV. Instead, the TDA predicts a large red shift (~ 1 eV) of the transverse plasmon mode, in striking disagreement with the experiment.

Similarly to the case of the *trans*-azobenzene molecule, the theoretical results dramatically worsen when the TDA is used to solve the BS equation. The full solution of the BS Hamiltonian predicts the 6 eV main peak to blue shift by 0.5 eV when going from parallel to perpendicular light polarization, thus well reproducing the trend observed experimentally.²⁷ Instead the TDA predicts the main peak appearing in the case of parallel polarized light to be at 8 eV, and more importantly it induces a 1 eV red shift in the case of perpendicular polarized light in stark disagreement with experimental evidence.

In order to rationalize the reason behind the TDA breakdown, in Figure 3 we analyze the absorption $\mathcal{A}(\epsilon)$ (left stack) and zero momentum EEL $-\mathcal{A}(\epsilon^{-1})$ (right stack) spectra of CNT calculated within the BS equation as a function of the angle ϕ that the perturbing field forms with the tube axis. We compare the full solution of the BS equation (full line) with the result of the TDA (dashed line).

For a parallel perturbing field ($\phi = 0^\circ$), the CNT behaves as an extended solid. As expected, in this case the TDA well describes the excitonic peaks in the absorption spectrum.^{6,25} On the contrary the TDA completely fails in reproducing the longitudinal plasmonic peak in the EEL spectrum, overestimating its frequency by 1.5 eV. By increasing the ϕ angle, the perturbing field acquires a perpendicular compo-

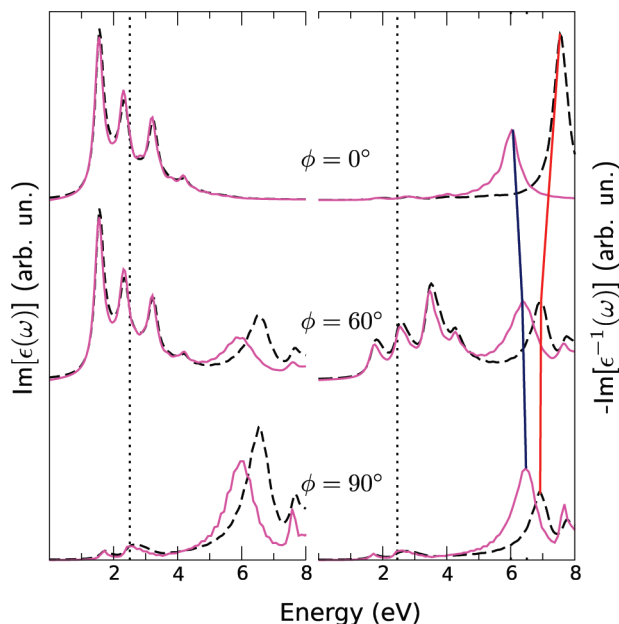


Figure 3. Polarized (angle ϕ with respect to the CNT axis) absorption (left stack) and ϕ -dependent EEL (right stack) spectra of zigzag (8,0) CNT calculated within the BS equation either by using the full (solid line) or the TDA (dashed line) Hamiltonian. The dotted line indicates the position of the quasiparticle band gap.⁶ In the EEL spectra (right stack), the blue and red lines highlight the angular dependence of the main peak at ~ 6 eV for the full Hamiltonian and TDA respectively. Going from $\phi = 0^\circ$ to $\phi = 90^\circ$ the peak is red shifted by about 1 eV within the TDA while is blue shifted by about 0.5 eV in the full Hamiltonian. See also Figure 2.

nent, and a peak at ~ 6 eV appears in the $\epsilon(\omega)$ function. The very same peak occurs in the EEL spectrum, confirming that it corresponds to a mixed excitonic-plasmonic excitation. This mixed behavior is misdescribed by the TDA both in the absorption and in the EEL spectra. The TDA performs even worse for a transverse perturbing field ($\phi = 90^\circ$), where the excitations are confined within the tube radius. The $\epsilon(\omega)$ and $\epsilon^{-1}(\omega)$ functions become very similar, that is, the system behaves as an isolated molecule. Thus, like in the case of the *trans*-azobenzene molecule, the contribution from e - h antipairs cannot be neglected, and the TDA yields an error on the position of the main peak in the absorption/EEL spectra of ~ 0.6 eV.

In summary, we have shown that in contrast to the common belief, the excitations appearing in the absorption spectrum of nanoscale systems (like CNTs and molecules) are not all purely excitonic. In particular, the analysis of the light polarization dependence of the CNT absorption and EEL spectra reveal how pure excitons gradually acquire a plasmonic character. The major consequence of this peculiar behavior is to make the widely used TDA inadequate. Indeed, we have shown that the TDA breaks down where dimensionality effects confine the optical excitation, inducing a mixed excitonic-plasmonic behavior. As clear instances of the TDA breakdown we have presented the polarizability of the *trans*-azobenzene molecule and the response properties of CNTs. For the *trans*-azobenzene molecule the TDA blue-shifts the spectrum by ~ 0.2 eV with respect to the experiment. For the CNTs, the TDA cannot even qualitatively

reproduce the polarization dependence of the EEL and the photoabsorption cross section spectra in the UV region.

We propose a novel approach to solve the BS (and time-dependent density functional theory) equation beyond the TDA, keeping the numerical advantages of a Hermitian formulation. This approach successfully explains the polarizability of *trans*-azobenzene molecule and the polarization dependence in the optical and EEL spectra of CNTs and opens the way to a truly ab initio approach to linear response properties of nanoscale materials.

Acknowledgment. This work was supported by the EU through the FP6 Nanoquanta NoE (NMP4-CT-2004-50019), the FP7 ETSF I3 e-Infrastructure (Grant Agreement 211956), the Belgian Interuniversity Attraction Poles Program (P6/42), the Communauté Française de Belgique (ARC 07/12-003), and the Région wallonne (WALL-ETSF).

References

- (1) Salpeter, E. E.; Bethe, H. A. *Phys. Rev.* **1951**, *84*, 1232.
- (2) Fetter A. L. Walecka J. D. *Quantum Theory of many-particle systems*; Dover: Mineola, NY, 2003; Chapter 15, p 565.
- (3) *Templates for the solution of algebraic problems: a practical guide*; Bai, Z., Demmel, J., Dongarra, J., Ruhe, A., van der Vorst, H., Eds.; SIAM: Philadelphia, PA, 2000.
- (4) Olevano, V.; Reining, L. *Phys. Rev. Lett.* **2001**, *86*, 5962.
- (5) See, for example: (a) Del Puerto, M.; et al. *Phys. Rev. Lett.* **2006**, *97*, 096401. (b) Arnaud, B.; et al. *Phys. Rev. Lett.* **2006**, *96*, 026402. (c) Wirtz, L.; et al. *Phys. Rev. Lett.* **2006**, *96*, 126104.
- (6) Spataru, C. D.; et al. *Top. Appl. Phys.* **2008**, *111*, 195.
- (7) Hirata, S.; Head-Gordon, M. *Chem. Phys. Lett.* **1999**, *314*, 291.
- (8) Onida, G.; et al. *Rev. Mod. Phys.* **2002**, *74*, 601.
- (9) Runge, E.; Gross, E. K. U. *Phys. Rev. Lett.* **1984**, *52*, 997.
- (10) (a) The GW_0 quasiparticle corrections and the BS spectra are calculated with the yambo code (Marini, A.; Hogan, C.; Grüning, M.; Varsano, D. *Comput. Phys. Commun.* **2009**, *180*, 1392), where the algorithm proposed in this work has been implemented. (b) The Kohn-Sham basis (local density approximation) is calculated with ABINIT, Gonze, X.; et al. *Comput. Mater. Sci.* **2002**, *25*, 478. (c) Gonze, X.; et al. *Z. Kristallogr.* **2005**, *220*, 478.
- (11) We have calculated the quasiparticle (QP) corrections for the five highest occupied and four lowest unoccupied states using the GW approximation (GW gap 6.9 eV). Five hundred states have been included to calculate the plasmon pole dielectric function $\epsilon_{GG'}$ (2 Ha cut-off) and the Green function. The energies of the Green functions have been updated up to self consistence (using a linear extrapolation for the QP corrections not explicitly computed). In the calculation for

the BS spectrum, we included all e-h pairs from the 18 highest occupied and 85 lowest unoccupied states. Two hundred states instead have been included in the static polarization function. We used a cutoff of 0.5 Ha for the screened interaction and of 3 Ha for the exchange component.

- (12) (a) *NIST Chemistry WebBook*; <http://webbook.nist.gov/chemistry> (accessed February 5, 2009). den Hertog, H. J.; Henkens, C. H.; van Roon, J. H. *Recl. Trav. Chim.* **1952**, *71*, 1145. Note that the experimental spectrum is scaled so that the height of the most intense peak coincides with that of the full Hamiltonian calculated spectrum.
- (13) As a consequence of the difference in the relative intensity of the peaks between the TDA and the full Hamiltonian, the static polarizability $\mathcal{A}[\alpha(\omega = 0)]$ is also affected. Indeed, the TDA underestimates $\mathcal{A}[\alpha(\omega = 0)]$ by about 15% with respect to the full Hamiltonian.
- (14) Mostafazadeh, A. *J. Math. Phys.* **2002**, *43*, 3944.
- (15) Zimmermann, R. *Phys. Status Solidi* **1970**, *41*, 23.
- (16) Mostafazadeh, A. *J. Math. Phys.* **2002**, *43*, 205.
- (17) When the formation of excitons does not lead to a fundamental change of ground state, \bar{H} is positive definite, see ref 15.
- (18) Haydock, R. In *Solid State Physics*; Ehrenfest, H., Seitz, F., Turnbull, D., Eds.; Academic Press, New York, 1980; Vol. 35, pp 215–294.
- (19) Benedict, L. X.; Shirley, E. L. *Phys. Rev. B* **1999**, *59*, 5441.
- (20) Because of the interplay between H , F and \bar{H} , evaluating the \bar{H} -inner product does not require extra operation with respect to the standard inner-product.
- (21) The proposed approach requires mN^2 operations, where m is the number of iterations and N the size of the system. For azobenzene $N \sim 10^4$ and $m \sim 10^2$. Thus, it is much faster and convenient compared to the standard diagonalization, that requires $O(N^3)$ operations.
- (22) O'Connell, M. J.; Bachilo, S. M.; Huffman, C. B.; et al. *Science* **2002**, *297*, 593.
- (23) Murakami, Y.; et al. *Phys. Rev. Lett.* **2005**, *94*, 087402.
- (24) Kramberger, C.; et al. *Phys. Rev. Lett.* **2008**, *100*, 196803.
- (25) (a) Chang, E.; Busi, G.; Ruini, A.; Molinari, E. *Phys. Rev. Lett.* **2004**, *92*, 196401. (b) Spataru, C. D.; Ismail-Beigi, S.; Benedict, L. X.; Louie, S. G. *Phys. Rev. Lett.* **2004**, *92*, 077402. (c) Deslippe, J.; Spataru, C. D.; Prendergast, D.; Louie, S. G. *Nano Lett.* **2007**, *7*, 1626.
- (26) We have included e-h pairs and antipairs from band 32 to 96 in a window of 15 eV and used cut-offs of 4 and 1 Ha for the \bar{V} and W integrals. The 1D Brillouin zone is sampled by 64 k-points. Quasiparticle correction from ref 6.
- (27) Note that our system differs from the experimental one. The latter is far more complex and thus cannot be treated using ab initio methods. In fact, the experimental system consists of a film of aligned bundles of CNTs with an average diameter of 2 nm. In particular the different diameter [2 nm versus ~ 0.6 nm of the (8,0) zig-zag CNT] explains the different position of the spectrum onset (the gap is known to decrease with the tube diameter). In spite of these differences, within the full Hamiltonian formulation, the BS equation reproduces well the polarization dependence of the observed photoabsorption spectra.

NL803717G